Review

Behçet's syndrome patients exhibit specific microbiome signature

CrossMark

Clarissa Consolandi [a],[*],[1], Silvia Turroni [b],[1], Giacomo Emmi [c],[1], Marco Severgnini [a], Jessica Fiori [b], Clelia Peano [a], Elena Biagi [b], Alessia Grassi [c], Simone Rampelli [b], Elena Silvestri [c], Manuela Centanni [b], Fabio Cianchi [e], Roberto Gotti [b], Lorenzo Emmi [d],[**], Patrizia Brigidi [b], Nicola Bizzaro [f], Gianluca De Bellis [a], Domenico Prisco [c],[d], Marco Candela [b], Mario M. D'Elios [c],[d]

[a] Institute of Biomedical Technologies, National Research Council (ITB-CNR), Segrate, Milan, Italy
[b] Department of Pharmacy and Biotechnology, University of Bologna, Bologna, Italy
[c] Department of Experimental and Clinical Medicine, University of Florence, Florence, Italy
[d] Medical Pathology, Center for Autoimmune Systemic Diseases, Behçet Center and Lupus Clinic, AOU Careggi, Florence, Italy
[e] Department of Surgery and Translational Medicine, University of Florence, Italy
[f] Laboratory of Clinical Pathology, Diagnostic Department, San Antonio Hospital, Tolmezzo, Italy

ARTICLE INFO

ABSTRACT

Background and aims: Behçet syndrome is a systemic inflammatory condition characterized by muco-cutaneous and ocular manifestations, with central nervous system, vascular and/or gastro-intestinal involvement. The association of microbiota with Behçet syndrome has not been shown yet. Our work was aimed to compare the gut microbiota structure and the profiles of short-chain fatty acids production in Behçet syndrome patients and healthy control relatives.
Methods: Here, we compared the fecal microbiota of 22 patients with Behçet syndrome and that of 16 healthy cohabiting controls, sharing the same diet and lifestyle by pyrosequencing of the V3–V4 hypervariable regions of the 16 rDNA gene and biochemical analyses.
Results: Our analyses showed significant differences in gut microbiota between Behçet patients and healthy cohabitants. In particular we found that Behçet's patients were significantly depleted in the genera *Roseburia* and *Subdoligranulum*. *Roseburia* showed a relative abundance value of $10.45 \pm 6.01\%$ in healthy relatives and $4.97 \pm 5.09\%$ in Behçet's patients, and *Subdoligranulum*, which reached a relative abundance of $3.28 \pm 2.20\%$ in healthy controls, was only at $1.93 \pm 1.75\%$ of abundance in Behçet's patients. Here we report, for the first time, that a peculiar dysbiosis of the gut microbiota is present in patients with Behçet syndrome and this corresponds to specific changes in microbiome profile. A significant decrease of butyrate production ($P = 0.0033$) in Behçet's patients was demonstrated. Butyrate is able to promote differentiation of T-regulatory cells, and consequently the results obtained prompt us to speculate that a defect of butyrate production might lead to both reduced T-reg responses and activation of immuno-pathological T-effector responses.
Conclusions: Altogether, our results indicate that both a peculiar dysbiosis of the gut microbiota and a significant decrease of butyrate production are present in patients with Behçet syndrome.

Contents

1. Introduction

Behçet syndrome (BS) is a systemic vasculitis characterized by muco-cutaneous and ocular manifestations, with central nervous system, vascular and gastro-intestinal involvement [1,2]. BS is common in the Middle East, Mediterranean countries, Asia, and Japan, whereas it is quite rare in the United States and Northern European countries [3, 4]. To date diagnosis is only based on clinical criteria as no sensitive and specific relevant biological tests are available [5,6]. It has been reported that carrying the human leukocyte antigen (HLA)-B51 increases the risk of developing BS by 1.5 to 16 times [7–9]; however, except for the severity of ocular disease [10], HLA-B51 does not seem to be correlated with the prognosis of BS. The exact cause of BS remains unknown but it is believed that both genetic and environmental factors contribute to the development of the disease [11,12], by the interaction between genetic background and infectious agents that might concur to the immune dysregulation [13–16]. A role of oral flora has also been considered in the etiopathogenesis of BS given the high frequency of oral ulcers [4]. The activation of innate immune responses by pathogens, and the consequent interaction between activated T-cells with neutrophils, can determine tissue damage and vasculitis in BS [17,18].

The human gut microbiota (GM) – the enormous community of symbiont microorganisms inhabiting our gut – has been recognized as a key factor for human health and homeostasis [19,20]. The role of GM in our physiology is so profound that human beings have been reconsidered as super-organisms, as a result of millennia of co-evolution with their microbial counterpart [21]. Even if the main evolutionary force shaping the GM–host mutualism has been the microbiome-dependent increase of energy extraction from food [22,23], the recent adoption of germ-free mouse models allowed to disclose several aspects of the human biology which rely on the mutualistic interaction with our "microbial organ," such as the energetic homeostasis [24], the estrogen equilibrium [25] and the function of the immune system [26]. In particular, GM is an active component of our immune system, being essential for immune education during the early life and for the maintenance of the immune homeostasis during the entire life course [27,28]. Short chain fatty acids (SCFAs) – butyrate, propionate and acetate – are the downstream mediators of the GM anti-inflammatory activity, showing a pivotal role in the immunological cross-talk with the host [29]. The concerted action of these three metabolites is the endpoint of GM community fermentation processes in the gut and is fundamental to preserve immune homeostasis and functionality of the host immune system [30]. In particular, it has been shown in mice that GM is able to dictate the type of T-cell responses elicited in the host [31,32]. Current evidence indicates that GM is important in health and diseases, including gastroenterologic, autoimmune, and even neuropsychiatric disorders [33–35].

While a mutualistic SCFA-producing GM configuration is a key factor to preserve the human health, GM dysbioses toward a pro-inflammatory layout have been implicated in the onset, progression and consolidation of several immune disorders, such as inflammatory bowel disease (IBD), colorectal cancer, type II diabetes and allergy [20,27,36]. It has been also hypothesized that an impaired microbiome–host interaction might contribute to the genesis of BS [37].

The aim of this study was to compare the GM structure and the profiles of SCFA production in BS patients and healthy control relatives eating the same diet and living in the same environment of BS patients. Here, we report that a peculiar dysbiosis of the gut microbial ecosystem is present in patients with BS, corresponding to specific changes in the profiles of SCFA production; in particular a significant decrease of butyrate production in Behçet's patients was demonstrated. Interestingly butyrate is able to induce T regulatory cell (Treg) differentiation via several mechanisms, thus influencing immune regulation [38] probably promoting an abnormal immune system response.

Altogether, the results obtained in this study lead us to speculate that novel diet- and/or probiotic-based strategies specifically tailored to the manipulation of the intestinal dysbiosis in BS might be useful for both prevention and treatment of the disease.

2. Methods

2.1. Subject enrolment and sample collection

In the present study 38 subjects were enrolled, including 22 patients with BS (12 males and 10 females; mean age, 41.1 years) attending the Florence Behçet Center and 16 age-matched healthy controls (6 males and 10 females; mean age 43.4 years). All participants had a comparable lifestyle in the last 6 months, in particular the same Mediterranean diet, without assumption of probiotics or antibiotics. Healthy controls of the study lived in the same house of BS patients: in 5 cases the control was a first-degree relative, while in the other 11 a cohabitant. Participants who had other diseases, such as autoimmune disorders, infections or malignancies, that might affect the outcome were excluded from the study.

All the patients were diagnosed as BS according to ISGC, the mean duration of illness was between 11 months and 27 years and 50% of them showed a HLA-B51 serotype. Oral aphthosis was present in all patients, followed by genital ulcers (63.5%), articular involvement (50%), cutaneous manifestations (35%), intestinal symptoms with or without endoscopic lesions (32%), vascular involvement (30%) and ocular impairment (29%); only 13% of patients presented central nervous system involvement (Fig. S1). Pathergy test was positive in 5 of 22 patients.

The study protocol was approved by the Ethical Committee of Azienda Ospedaliero-Universitaria (AOU) Careggi, Florence, Italy. Informed consent was obtained from all subjects.

2.2. Microbial DNA extraction from feces

Total bacterial DNA from fecal material was extracted using the QIAamp DNA Stool Mini Kit (QIAGEN, Valencia, CA, USA) with a

modified protocol [39]. Briefly, 250 mg of feces was suspended in 1 ml of lysis buffer (500 mM NaCl, 50 mM Tris–HCl pH 8, 50 mM EDTA, 4% SDS) and 3 times bead-beaten with four 3-mm glass beads and 0.5 g of 0.1-mm zirconia beads (BioSpec Products, Bartlesville, OK, USA) in a FastPrep-24 Instrument (MP Biomedicals, Santa Ana, CA, USA) at 5.5 m/s for 1 min. After incubation at 95 °C for 15 min and centrifugation at full speed for 5 min to pellet stool particles, 260 μl of 10 M ammonium acetate was added to the supernatant, followed by incubation in ice for 5 min and centrifugation for 10 min. One volume of isopropanol was added to each sample and incubated in ice for 30 min. Precipitated nucleic acids were washed with 70% ethanol, resuspended in 100 μl of TE buffer and treated with 2 μl of DNase-free RNase (10 mg/ml) at 37 °C for 15 min. Each DNA sample was further treated with Proteinase K and purified with QIAamp Mini Spin columns (QIAGEN) following the manufacturer's instructions. DNA concentration and quality for each sample were determined using a NanoDrop ND-1000 spectrophotometer (NanoDrop Technologies, Wilmington, DE, USA).

2.3. 16S rRNA gene amplification

For the amplification of the V4 region of the 16S rRNA gene the primer set 520F (5′-AYTGGGYDTAAAGNG-3′) and 802R (5′-TACNVGGGTATCTAATCC-3′) (with Y = C/T, D = A/G/T, N = any base, V = A/C/G) [40] was utilized. Primers included at their 5′ end an adaptor sequence used in the 454-sequencing library preparation protocol, linked to a unique MID tag barcode of 10 bases that allowed the identification of the different samples. Amplifications were carried out in 50-μl final volume reaction mixtures containing 0.5 μM of each forward and reverse primer, together with 100 ng of template DNA, 2.5 U of GoTaq Flexi Polymerase (Promega, Madison, WI, USA), 200 μM of dNTPs and 2 mM of MgCl$_2$. Samples were initially denatured at 95 °C for 5 min, followed by 35 cycles of 94 °C for 50 s, 40 °C for 30 s, and 72 °C for 60 s, with a final extension step at 72 °C for 5 min [41]. PCR amplifications were performed in a Biometra Thermal Cycler T Gradient (Biometra, Goettingen, Germany).

2.4. Pyrosequencing

16S rRNA gene V4 hypervariable region amplicons were individually purified with MinElute PCR Purification Kit (QIAGEN) and, then, quantified using the Quant-iT PicoGreen dsDNA kit (Invitrogen, Carlsbad, CA, USA). After the individual quantification step, amplicons were pooled in equal amounts (creating four 6-plex and two 7-plex pools) and again purified by 454-Roche Double Ampure size selection protocol with Agencourt AMPure XP DNA purification beads (Beckman Coulter Genomics GmbH, Danvers, MA, USA) in order to remove primer dimers, according to the manufacturer's instructions (454 LifeSciences, Roche, Branford, CT, USA). Before emulsion PCR, purified amplicon pools were quantified using a quantitative Real Time PCR (qPCR) by KAPA Library Quant Kits (KAPA Biosystems, Wilmington, MA, USA). Afterwards, pools were fixed to microbeads to be clonally amplified by emulsion PCR following the GS-FLX protocol Titanium emPCR LIB-A (454 LifeSciences, Roche). Following this amplification step, beads were enriched in order to keep only those carrying identical PCR products on their surface, and loaded onto a picotiter plate for pyrosequencing reactions, following the GS-FLX Titanium sequencing protocol. Each pool was sequenced in one eighth of a plate.

2.5. SCFA analysis

For the extraction of SCFAs the method described in Schnorr et al. [41] was followed. Briefly, 250 mg of fecal samples were extracted by adding 1 ml of 10% perchloric acid in water and centrifuged at 15,000 g for 5 min at 4 °C. Fifty microlitres of supernatant were diluted 1:10 in water, 10 μl of D8-butyric acid (internal standard, IS) were added to the sample at the final concentration of 20 μg/ml. The sample was stirred for 10 min at 70 °C to reach the equilibrium of volatile compounds between the matrix and the headspace. Then, SCFA extraction was performed by using a 75-μm Carboxen/polydimethylsiloxane fiber (Supelco, Sigma-Aldrich, St. Louis, MO, USA) for 30 min at 70 °C. After extraction, samples were directly desorbed into the gas chromatograph (GC) injection port at 250 °C for 10 min, including fiber cleaning. The GC–mass spectrometry (GC–MS) analysis was performed on a TRACE GC 2000 Series (ThermoQuest CE Instruments, Waltham, MA, USA), interfaced with GCQ Plus (ThermoQuest CE Instruments) mass detector with ion trap analyzer, operating in EI mode (70 eV). The GC was operated in splitless mode; the injector base temperature was set at 250 °C. The capillary GC column was a Phenomenex ZB-WAX (30 m × 0.25 mm ID, 0.15 μm film thickness), consisting of 100% polyethylene glycol. Helium (He) was the carrier gas at a flow rate of 1.0 ml/min. An oven temperature program was adopted: initial 40 °C (hold time: 5 min), and then ramped by 10 °C/min to 220 °C (hold time: 5 min). The temperature of transfer line and ionization source was maintained at 250 °C and 200 °C, respectively. The mass spectra were recorded in full scan mode (34–200 a.m.u.) to collect the total ion current chromatograms. The compounds were identified by comparison of retention time and mass spectra with those of commercial reference standards provided by Sigma-Aldrich. Quantification was carried out by using the extracted ion chromatograms by selecting fragment ions of the studied analytes (43 and 60 a.m.u. for acetic acid, 55 and 73 a.m.u. for propionic acid, 60 and 73 a.m.u. for butyric and valeric acids, and 63 and 77 a.m.u. for IS). The SCFA concentration in fecal samples was expressed in μmol/g of feces. Limit of detection ranged from 4 to 68 nmol/g.

All the standards (purity >99%), acetic, propionic, butyric, valeric acids and IS were provided by Sigma-Aldrich and were used to prepare calibration solutions for quantification (linear response). The calibration curves were prepared by adding the IS to scalar amounts of the acids in water or diluted samples (for external standardization and recovery).

2.6. Bioinformatic analysis and statistical data analysis

Sequencing reads were analyzed using the QIIME pipeline [42] as described previously [41]. Briefly, pyrosequencing V4 reads were filtered according to the following criteria: (i) read length between 150 bp and 350 bp; (ii) no ambiguous bases (Ns) in the reads; (iii) a minimum average quality score of 25 over a 50-bp rolling window; (iv) exact match to primer sequences and maximum 1 error in barcode tags. Trimmed reads were clustered into OTUs at 97% identity level, aligned against the Greengenes database [43] by PyNAST algorithm and filtered for chimeric sequences using ChimeraSlayer (http://microbiomeutil.sourceforge.net/#A_CS). RDP-classifier (version 2.2) with 50% confidence value threshold was used for bacterial taxonomy assignment. Alpha-diversity and rarefaction plots were computed using Shannon, PD whole tree, chao1 and observed species metrics. Statistical evaluation of differences in alpha-diversity indices was performed by a non parametric, Monte Carlo-based test, using 9999 random permutations. Principal coordinates analysis (PCoA) was performed using both weighted and unweighted UniFrac distances, and data separation was tested using a permutation test with pseudo F-ratios (adonis test with pseudo F-ratios on 9999 permutations). Hierarchical clustering using Spearman rank correlation distance and average linkage, and heatmaps were performed on relative abundance (rel. ab.) values at family level in TMeV 4.6.2 [44]. Statistical analysis of GM differences between BS patients and controls was performed in Matlab (MathWorks, Natick, MA. USA), using a Wilcoxon signed rank test. The Kendall correlation test between SCFA levels and the relative abundance of genera was achieved using function "cor.test" of the package "Stats" of R. In all statistical tests, a p-value < 0.05 was considered as significant.

3. Results

3.1. Intestinal microbiota in Behçet's patients

GM structure from 22 Behçet's patients and 16 healthy relatives, belonging to 21 different families (Table S1), was characterized by mean of pyrosequencing of the V4 region of the bacterial 16S rRNA gene (Fig. S2a,b,c). A total of 261,958 high-quality reads were obtained, with a mean of $6{,}893 \pm 2{,}673$ reads (range 2760–12,581) per subject. Reads were clustered in 7652 operational taxonomic units (OTUs) at 97% of identity. OTU rarefaction curves based on number of unique OTUs, Shannon, Chao1 and phylogenetic diversity metrics reached the plateau after about 2500 reads (Fig. S3), suggesting that the depth of coverage we accomplished was sufficient to capture nearly the entire biological diversity within samples.

The GM of both BS patients and healthy controls was largely dominated by Firmicutes (relative abundance (rel. ab.) $86.0 \pm 10.9\%$ and $88.4 \pm 6.8\%$, respectively), Actinobacteria (rel. ab. $5.9 \pm 9.3\%$ and $5.8 \pm 6.5\%$, respectively) and Bacteroidetes (rel. ab. $6.8 \pm 5.0\%$ and $5.1 \pm 3.8\%$, respectively).

The most represented families in gut microbial communities were *Ruminococcaceae* (rel. ab. $31.9 \pm 11.9\%$ and $34.9 \pm 9.3\%$ in BS and controls, respectively), *Lachnospiraceae* (rel. ab. $21.9 \pm 9.8\%$ and $25.1 \pm$ 7.0%, respectively), *Clostridiales* (rel. ab. $10.5 \pm 5.9\%$ and $7.1 \pm 3.0\%$, respectively), *Clostridiales* Incertae Sedis XIV (rel. ab. $13.3 \pm 9.5\%$ and $12.6 \pm 5.8\%$, respectively), *Bifidobacteriaceae* (rel. ab. $5.7 \pm 9.2\%$ and $5.6 \pm 6.5\%$, respectively) and *Bacteroidaceae* (rel. ab. $4.2 \pm 4.6\%$ and $2.2 \pm 1.3\%$, respectively). Subdominant families showing rel. ab. values below 5% were: *Erysipelotrichaceae*, *Eubacteriaceae*, *Rikenellaceae*, *Porphyromonadaceae*, and *Enterobacteriaceae* (Fig. S2b).

3.2. Comparison between GM communities in Behçet's patients and healthy relatives

In order to highlight GM dysbiosis signatures of BS, a detailed comparative analysis of the GM communities in Behçet's patients and healthy relatives was performed. At first, we sought the degree of intrasubject GM diversity in the two groups. Interestingly, comparison of rarefaction curves indicated a reduced diversity for the gut microbial community in BS (Fig. 1). Confirming this observation, community richness comparison by using different metrics – Shannon diversity, Chao1, observed species and PD whole tree – always showed a significantly ($P <$ 0.01) lower degree of α-diversity in the BS gut microbial ecosystem respect to healthy controls (Table S2). To investigate the degree of intersubject GM diversity (β-diversity) in our study cohort, we calculated unweighted and weighted UniFrac phylogenetic distances of the GM
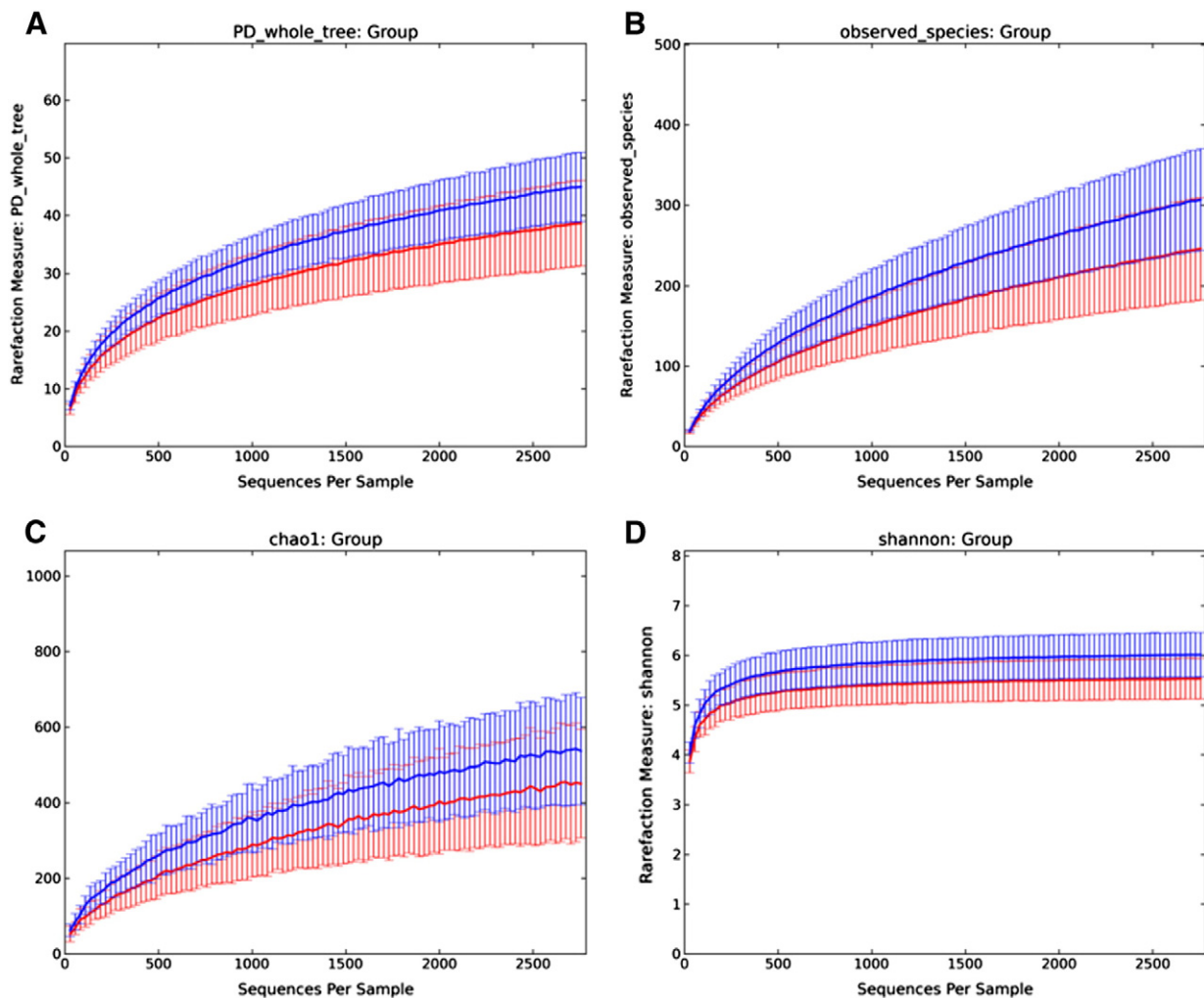
Fig. 1. α-Diversity rarefaction curves for the 16S rRNA V4 region pyrosequencing reads. Average indexes (plus standard error bars) for the phylogenetic diversity whole tree (PD_whole_tree, A), observed species (B), Chao1 (C) and Shannon diversity (D) are reported for the Behçet (red line, $n = 22$) and control (blue line, $n = 16$) groups. X-axis reports the number of sequences per sample used for the calculation. Curves were built calculating the average diversity index on 10 random extractions for 100 linearly spaced sampling points between 27 to 2700 sequencing reads.

composition among subjects. According to our findings, the PCoA representation of both unweighted and weighted UniFrac distances resulted in the separation of Behçet's patients and healthy controls (Fig. 2), with significant values obtained with unweighted UniFrac distance metrics ($P = 0.0114$), suggesting that the differences between the two subject groups likely involved a subdominant fraction of the GM. Average β-diversity indexes among the samples coming from Behçet or control group indicated no difference but comparable levels of β-diversity between the two study groups (average β-diversity for unweighted UniFrac distances: 0.68 ± 0.16 in Behçet's patients and 0.65 ± 0.17 in controls; average β-diversity for weighted UniFrac distances: 0.59 ± 0.17 in Behçet's patients and 0.52 ± 0.18 in controls).

In Table 1 we report phylum- to genus-level differences between GM from Behçet's patients and healthy relatives. While no significant difference at the level of phylum was found, Behçet's patients were significantly depleted in the dominant GM genera *Roseburia* and *Subdoligranulum*, which belong to the *Clostridium* clusters XIVa and IV, respectively. In particular, *Roseburia* showed a rel. ab. value of $10.45 \pm 6.01\%$ in healthy relatives and $4.97 \pm 5.09\%$ in Behçet's patients, and *Subdoligranulum*, which reached a rel. ab. of $3.28 \pm 2.20\%$ in healthy controls, was only at $1.93 \pm 1.75\%$ of abundance in Behçet's patients. Interestingly, the unsupervised hierarchical clustering at family level did not show sample separation either according to BS status or degree of kinship (Fig. S4), suggesting that the GM dysbioses associated to BS overcame intrinsic GM similarities among individuals of the same family, although differences were not enough to show a clear separation according to disease state of the samples.

3.3. SCFA profiles

The abundance of SCFAs in stool samples from Behçet's patients and healthy relatives was determined by GC–MS (Table S3). The PCoA of the individual SCFA profiles showed a significant ($P = 0.0339$) segregation between Behçet's patients and healthy relatives (Fig. 3). In particular, Behçet's patients were characterized by a significant reduction of butyrate ($P = 0.0033$) and a tendency toward a corresponding increase in acetate ($P = 0.068$) (Fig. S5). No difference, on the other side, was observed for propionate.

In order to dissect whether the major dysbioses of the GM structure of Behçet's patients could have an impact on their peculiar profile of SCFAs, Kendall correlation values between *Roseburia* and *Subdoligranulum* – both significantly reduced in Behçet's patients – and acetate, propionate and butyrate were calculated. Interestingly, *Roseburia* showed a

tendency ($P = 0.073$) toward a positive association with butyrate (Kendall correlation = 0.207). Differently, *Subdoligranulum* did not result in any correlation with SCFAs.

4. Discussion

Based on the hypothesis that GM structure and function could affect the pathogenesis of BS, here we sought GM dysbioses in BS and the corresponding outcome in terms of microbiota–host trans-genomic metabolism. By comparing GM structure and SCFA content in Behçet's patients and healthy controls, we have successfully described peculiar distortions of the GM profile in BS, as well as the consequent impact in terms of pattern of SCFA production. In particular, the BS-associated GM was characterized by a significant reduction of the total bacterial diversity compared to a healthy intestinal ecosystem. Furthermore, a significant depletion of *Roseburia* and *Subdoligranulum* in the GM of Behçet's patients was observed. Belonging to the *Clostridium* clusters XIVa and IV, respectively, these microorganisms are well-known butyrate producers of the human GM and are generally associated with a healthy GM structure [45,46]. Strengthening these findings, we demonstrated a significant decrease of butyrate production in Behçet's patients.

Taken together, our data provide experimental evidence supporting a dysbiotic structure of the GM ecosystem in BS; characterized by a low biodiversity and by a depletion of key butyrate-producing members, the GM of Behçet's patients deviates from a mutualistic layout, resulting in an overall decrease of butyrate abundance in the gut. Butyrate is a key microbial metabolite in the context of the GM–host mutualism, with a well-consolidated role as a modulator of the host immune function. In particular, butyrate exerts an important role for the maintenance of the host immune homeostasis [30], showing both systemic and local immuno-modulating properties. In fact, while circulating butyrate prompts the generation of extrathymic Treg [47], gut butyrate has been reported to inhibit local pro-inflammatory cytokines [48]. The role of butyrate in host physiology goes beyond the immune function. In fact, butyrate represents the main energy source for colonocytes [49] and, stimulating the release of mucins, it also exerts a protective role strengthening the gut epithelial barrier [50].

T-lymphocytes producing interferon-γ and interleukin 17, together with neutrophils, are thought to represent the main effector cells in the pathogenesis of BS [37]. Interestingly, butyrate is able to promote differentiation of Treg via several mechanisms, thus influencing immune regulation and altering the mucosal immune response [38]; the
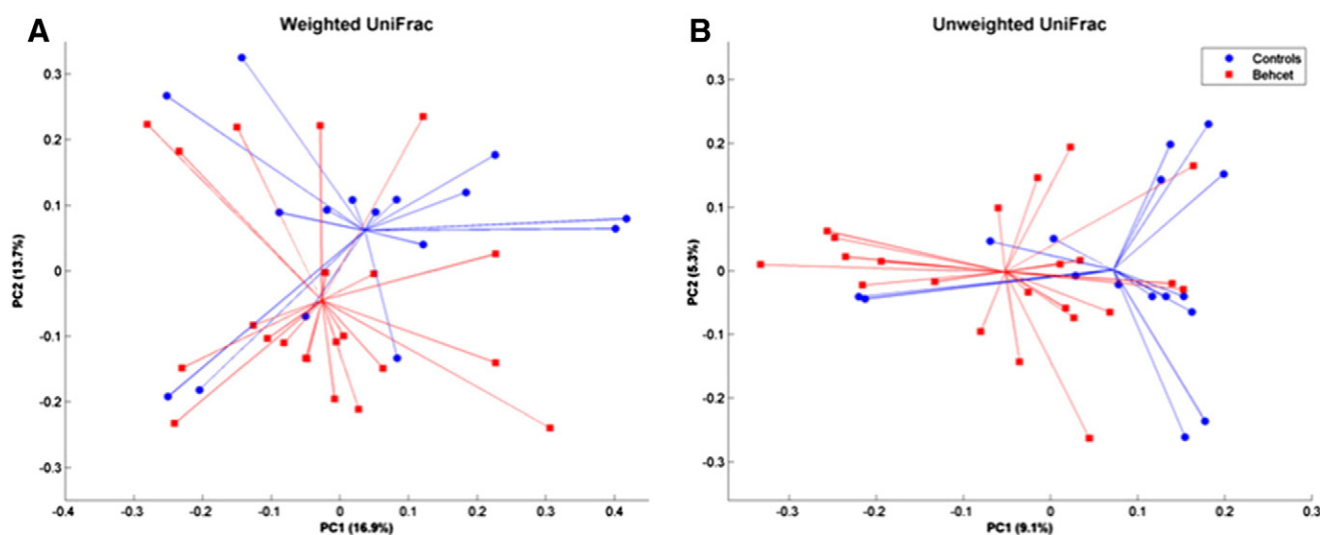

Fig. 2. Differences in GM structure between Behçet's patients and healthy relatives. PCoA of the weighted (A) and unweighted (B) UniFrac distances, represented according to belonging to Behçet (red squares) or control (blue circles) group. Percent variance accounted for by the first and second principal component (PC) is shown.

Table 1
List of taxonomic units enriched or depleted in the GM of Behçet's patients with respect to healthy relative controls. For each taxonomical group, the average relative abundance (plus standard deviation) and the P-value of the Mann–Whitney U-test between the two groups are reported. Only P-values < 0.3 are shown. .

Phylogenetic level	Taxonomy	Behçet Avg rel. ab. (st. dev)	Controls Avg rel. ab. (st. dev)	P-value[a]
Phylum	Bacteria; Lentisphaerae	0.00 (0.01)	0.00 (0.00)	0.236
	Bacteria; TM7	0.00 (0.01)	0.00 (0.00)	0.236
	Bacteria; Bacteroidetes	6.80 (5.04)	5.11 (3.84)	0.268
Class	Bacteria; Firmicutes; Bacilli	0.62 (0.65)	0.46 (0.74)	0.084
	Bacteria; Bacteroidetes; Sphingobacteria	0.01 (0.02)	0.00 (0.00)	0.137
	Bacteria; Lentisphaerae; Lentisphaeria	0.00 (0.01)	0.00 (0.00)	0.236
Order	Bacteria; Actinobacteria; Actinobacteria; Other	0.00 (0.00)	0.01 (0.02)	0.040[*]
	Bacteria; Proteobacteria; Deltaproteobacteria; Other	0.00 (0.00)	0.01 (0.02)	0.040[*]
	Bacteria; Firmicutes; Clostridia; Other	0.43 (1.53)	0.05 (0.10)	0.065
	Bacteria; Firmicutes; Bacilli; Lactobacillales	0.62 (0.65)	0.45 (0.74)	0.074
Family	Bacteria; Actinobacteria; Actinobacteria; Other; Other	0.00 (0.00)	0.01 (0.02)	0.040[*]
	Bacteria; Proteobacteria; Deltaproteobacteria; Other; Other	0.00 (0.00)	0.01 (0.02)	0.040[*]
	Bacteria; Firmicutes; Clostridia; Clostridiales; Other	10.49 (5.87)	7.10 (2.97)	0.043[*]
	Bacteria; Firmicutes; Clostridia; Other; Other	0.43 (1.53)	0.05 (0.10)	0.065
	Bacteria; Bacteroidetes; Bacteroidia; Bacteroidales; Other	0.32 (1.27)	0.03 (0.06)	0.073
Genus	Bacteria; Firmicutes; Clostridia; Clostridiales; Lachnospiraceae; Roseburia	4.97 (5.09)	10.45 (6.01)	0.004[**]
	Bacteria; Firmicutes; Clostridia; Clostridiales; Ruminococcaceae; Papillibacter	0.73 (1.02)	0.24 (0.39)	0.040[*]
	Bacteria; Actinobacteria; Actinobacteria; Coriobacteriales; Coriobacteriaceae; Asaccharobacter	0.01 (0.02)	0.02 (0.03)	0.040[*]
	Bacteria; Actinobacteria; Actinobacteria; Other; Other; Other	0.00 (0.00)	0.01 (0.02)	0.040[*]
	Bacteria; Proteobacteria; Deltaproteobacteria; Other; Other; Other	0.00 (0.00)	0.01 (0.02)	0.040[*]
	Bacteria; Firmicutes; Clostridia; Clostridiales; Other; Other	10.49 (5.87)	7.1 (2.97)	0.043[*]
	Bacteria; Firmicutes; Clostridia; Clostridiales; Ruminococcaceae; Subdoligranulum	1.93 (1.75)	3.28 (2.20)	0.049[*]
	Bacteria; Firmicutes; Clostridia; Clostridiales; Ruminococcaceae; Lactonifactor	1.24 (1.32)	0.59 (0.59)	0.053
	Bacteria; Firmicutes; Clostridia; Other; Other; Other	0.43 (1.53)	0.05 (0.10)	0.065
	Bacteria; Actinobacteria; Actinobacteria; Coriobacteriales; Coriobacteriaceae; Slackia	0.00 (0.00)	0.01 (0.01)	0.066
	Bacteria; Bacteroidetes; Bacteroidia; Bacteroidales; Other; Other	0.32 (1.27)	0.03 (0.06)	0.073
	Bacteria; Firmicutes; Clostridia; Clostridiales; Lachnospiraceae; Robinsoniella	0.14 (0.32)	0.05 (0.09)	0.074

[a] Mann–Whitney U-test.
[*] P < 0.05.
[**] P < 0.01.

butyrate impairment in BS patients could favor a reduced Treg-mediated control, thus promoting a powerful immuno-pathological T-cell responses. In our cohort of Behçet's patients the presence of HLA-B51 does not seem to be correlated to a specific GM profile.

Interestingly, GM dysbioses similar to the ones we detected in Behçet's patients have been previously observed in IBD, whose patients are generally characterized by a reduction of GM ecosystem diversity, the decrease of butyrate producers belonging to the *Clostridium* clusters IV and XIVa, and the corresponding decrease of butyrate production in the gut [29,51]. These deviations from a GM mutualistic structure have

been hypothesized to contribute to IBD onset and progression through the establishment of a self-sustained pro-inflammatory loop in the gut [52].

Providing evidence of characteristic GM deviations from a healthy profile in BS, our data open the perspective to a therapeutic manipulation of GM structure in Behçet's patients, specifically targeted to the recovery of a mutualistic layout. For instance, besides the usage of probiotics, the content of dietary fiber can be specifically modulated in order to favor the increase of butyrate producers in the gut. Accordingly it has been recently demonstrated that oral administration of butyrate in mice is able to both favor Treg differentiation and to ameliorate colitis [30,53].
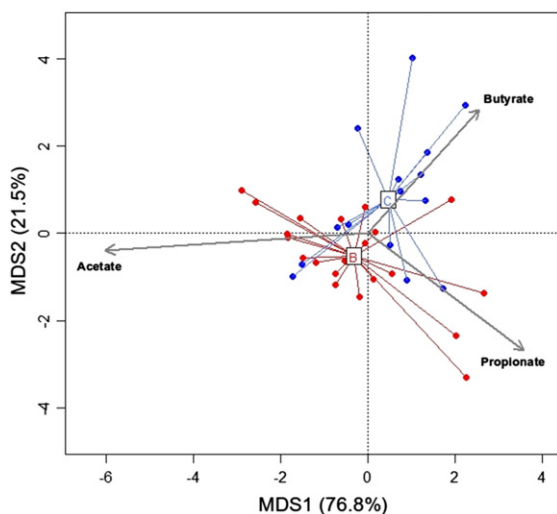
Supporting the recovery of a healthy pattern of SCFA production, these microorganisms could promote the immune homeostasis in BS, thus allowing the control of disease.

Disclosures

The authors disclose any actual or potential conflict of interest including any financial, personal or other relationships with other people or organizations within three years of beginning the submitted work that could inappropriately influence, or be perceived to influence, their work.

Fig. 3. Comparison of SCFA production between Behçet's patients and healthy relatives. PCoA based on Euclidean distances of the profiles of SCFA relative abundance in Behçet's patients (B, red dots) and healthy control relatives (C, blue dots). Percentage of variance explained by the first and second PC is reported.

Take home messages

- BS is a vasculitis with muco-cutaneous, ocular, and gastro-intestinal involvement.
- BS is associated to a peculiar dysbiosis of the gut microbial ecosystem.
- Gut microbiota ecosystem in BS is characterized by a low biodiversity.
- Behçet's patients were significantly depleted in the genera *Roseburia* and *Subdoligranulum*.
- BS patients show a decrease of butyrate production.
- The defect of butyrate production leads to reduced T-reg responses and activation of immuno-pathological T-effector responses.

Acknowledgements

Appendix A. Supplementary data

Supplementary data to this article can be found online at http://dx.doi.org/10.1016/j.autrev.2014.11.009.

References

[1] Mendoza-Pinto C, Garcia-Carrasco M, Jimenez-Hernandez M, Jimenez Hernandez C, Riebeling-Navarro C, Nava Zavala A, et al. Etiopathogenesis of Behcet's disease. Autoimmun Rev 2010;9:241–5.
[2] Emmi L. Behcet's syndrome — from pathogenesis to treatment. Heidelberg: Springer; 2014.
[3] Jennette JC, Falk RJ, Bacon PA, Basu N, Cid MC, Ferrario F, et al. 2012 Revised International Chapel Hill Consensus Conference nomenclature of vasculitides. Arthritis Rheum 2013;65:1–11.
[4] Sakane T, Takeno M, Suzuki N, Inaba G. Behcet's disease. N Engl J Med 1999;341:1284–91.
[5] International Study Group for Behçet's Disease. Criteria for diagnosis of Behçet's disease. Lancet 1990;335:1078–80.
[6] International Team for the Revision of the International Criteria for Behçet's Disease (ITR-ICBD), Davatchi F, Assaad-Khalil S, Calamia KT, Crook JE, Sadeghi-Abdollahi B, Schirmer M, et al. The International Criteria for Behçet's Disease (ICBD): a collaborative study of 27 countries on the sensitivity and specificity of the new criteria. J Eur Acad Dermatol Venereol 2014;28:338–47.
[7] de Menthon M, Lavalley MP, Maldini C, Guillevin L, Mahr A. HLA-B51/B5 and the risk of Behcet's disease: a systematic review and meta-analysis of case-control genetic association studies. Arthritis Rheum 2009;61:1287–96.
[8] Yazici H, Akokan G, Yalçin B, Müftüoğlu A. The high prevalence of HLA-B5 in Behcet's disease. Clin Exp Immunol 1977;30:259–61.
[9] Mizuki N, Inoko H, Ohno S. Pathogenic gene responsible for the predisposition of Behcet's disease. Int Rev Immunol 1997;14:33–48.
[10] Soylu M, Ersoz TR, Erken E. The association between HLA B5 and ocular involvement in Behcet's disease in southern Turkey. Acta Ophthalmol (Copenh) 1992;70:786–9.
[11] Chamorro AJ, Marcos M, Hernandez-Garcia I, Calvo A, Mejia JC, Cervera R, et al. Association of allelic variants of factor V Leiden, prothrombin and methylenetetrahydrofolate reductase with thrombosis or ocular involvement in Behcet's disease: a systematic review and meta-analysis. Autoimmun Rev 2013;12:607–16.
[12] Yazici H. The lumps and bumps of Behcet's syndrome. Autoimmun Rev 2004;3(Suppl. 1):S53–4.
[13] Mizushima Y, Matsuda T, Hoshi K, Ohno S. Induction of Behcet's disease symptoms after dental treatment and streptococcal antigen skin test. J Rheumatol 1988;15:1029–30.
[14] Mumcu G, Inanc N, Aydin SZ, Ergun T, Direskeneli H. Association of salivary S. mutans colonisation and mannose-binding lectin deficiency with gender in Behcet's disease. Clin Exp Rheumatol 2009;27:S32–6.
[15] Tojo M, Yanagihori H, Zheng X, Oyama N, Isogai E, Nakamura K, et al. Detection of microbial DNA in skin lesions from patients with Behcet's disease. Adv Exp Med Biol 2003;528:185–90.
[16] Yokota K, Hayashi S, Araki Y, Isogai E, Kotake S, Yoshikawa K, et al. Characterization of Streptococcus sanguis isolated from patients with Behcet's disease. Microbiol Immunol 1995;39:729–32.
[17] Zhou ZY, Chen SL, Shen N, Lu Y. Cytokines and Behcet's disease. Autoimmun Rev 2012;11:699–704.
[18] Pineton de Chambrun M, Wechsler B, Geri G, Cacoub P, Saadoun D. New insights into the pathogenesis of Behcet's disease. Autoimmun Rev 2012;11:687–98.
[19] Candela M, Biagi E, Maccaferri S, Turroni S, Brigidi P. Intestinal microbiota is a plastic factor responding to environmental changes. Trends Microbiol 2012;20:385–91.
[20] Neish AS. Microbes in gastrointestinal health and disease. Gastroenterology 2009;136:65–80.
[21] Gill SR, Pop M, Deboy RT, Eckburg PB, Turnbaugh PJ, Samuel BS, et al. Metagenomic analysis of the human distal gut microbiome. Science 2006;312:1355–9.
[22] Backhed F, Ding H, Wang T, Hooper LV, Koh GY, Nagy A, et al. The gut microbiota as an environmental factor that regulates fat storage. Proc Natl Acad Sci U S A 2004;101:15718–23.
[23] Koropatkin NM, Cameron EA, Martens EC. How glycan metabolism shapes the human gut microbiota. Nat Rev Microbiol 2012;10:323–35.
[24] De Vadder F, Kovatcheva-Datchary P, Goncalves D, Vinera J, Zitoun C, Duchampt A, et al. Microbiota-generated metabolites promote metabolic benefits via gut-brain neural circuits. Cell 2014;156:84–96.
[25] Plottel CS, Blaser MJ. Microbiome and malignancy. Cell Host Microbe 2011;10:324–35.
[26] Round JL, Mazmanian SK. The gut microbiota shapes intestinal immune responses during health and disease. Nat Rev Immunol 2009;9:313–23.
[27] Candela M, Biagi E, Turroni S, Maccaferri S, Figini P, Brigidi P. Dynamic efficiency of the human intestinal microbiota. Crit Rev Microbiol 2013:1–7.
[28] Centanni M, Turroni S, Consolandi C, Rampelli S, Peano C, Severgnini M, et al. The enterocyte-associated intestinal microbiota of breast-fed infants and adults responds differently to a TNF-alpha-mediated pro-inflammatory stimulus. PLoS One 2013;8:e81762.
[29] Atarashi K, Tanoue T, Oshima K, Suda W, Nagano Y, Nishikawa H, et al. Treg induction by a rationally selected mixture of Clostridia strains from the human microbiota. Nature 2013;500:232–6.
[30] Arpaia N, Campbell C, Fan X, Dikiy S, van der Veeken J, deRoos P, et al. Metabolites produced by commensal bacteria promote peripheral regulatory T-cell generation. Nature 2013;504:451–5.
[31] Ivanov II, Atarashi K, Manel N, Brodie EL, Shima T, Karaoz U, et al. Induction of intestinal Th17 cells by segmented filamentous bacteria. Cell 2009;139:485–98.
[32] Lee YK, Menezes JS, Umesaki Y, Mazmanian SK. Proinflammatory T-cell responses to gut microbiota promote experimental autoimmune encephalomyelitis. Proc Natl Acad Sci U S A 2011;108(Suppl. 1):4615–22.
[33] Ma HD, Wang YH, Chang C, Gershwin ME, Lian ZX. The intestinal microbiota and microenvironment in liver. Autoimmun Rev 2014;14:183–91.
[34] Severance EG, Yolken RH, Eaton WW. Autoimmune diseases, gastrointestinal disorders and the microbiome in schizophrenia: more than a gut feeling. Schizophr Res 2014. http://dx.doi.org/10.1016/j.schres.2014.06.027 [pii: S0920–9964(14)00319–3].
[35] Bogdanos DP, Smyk DS, Invernizzi P, Rigopoulou EI, Blank M, Pouria S, et al. Infectome: a platform to trace infectious triggers of autoimmunity. Autoimmun Rev 2013;12:726–40.
[36] Candela M, Rampelli S, Turroni S, Severgnini M, Consolandi C, De Bellis G, et al. Unbalance of intestinal microbiota in atopic children. BMC Microbiol 2012;12:95.
[37] D'Elios MM, Benagiano M, Amedei A, Emmi G. Infections, autoimmunity, and Behcet's syndrome: what liaison? Behcet's syndrome, Rare diseases of the immune system. Italia: Springer-Verlag; 2014.
[38] Kosiewicz M, Dryden G, Chhabra A, Alard P. Relationship between gut microbiota and development of T cell associated disease. FEBS Lett 2014;5793:224–5.
[39] Salonen A, Nikkila J, Jalanka-Tuovinen J, Immonen O, Rajilic-Stojanovic M, Kekkonen RA, et al. Comparative analysis of fecal DNA extraction methods with phylogenetic microarray: effective recovery of bacterial and archaeal DNA using mechanical cell lysis. J Microbiol Methods 2010;81:127–34.
[40] Claesson MJ, O'Sullivan O, Wang Q, Nikkila J, Marchesi JR, Smidt H, et al. Comparative analysis of pyrosequencing and a phylogenetic microarray for exploring microbial community structures in the human distal intestine. PLoS One 2009;4:e6669.
[41] Schnorr SL, Candela M, Rampelli S, Centanni M, Consolandi C, Basaglia G, et al. Gut microbiome of the Hadza hunter-gatherers. Nat Commun 2014;5:3654.
[42] Caporaso JG, Kuczynski J, Stombaugh J, Bittinger K, Bushman FD, Costello EK, et al. QIIME allows analysis of high-throughput community sequencing data. Nat Methods 2010;7:335–6.
[43] DeSantis TZ, Hugenholtz P, Larsen N, Rojas M, Brodie EL, Keller K, et al. Greengenes, a chimera-checked 16S rRNA gene database and workbench compatible with ARB. Appl Environ Microbiol 2006;72:5069–72.
[44] Saeed AI, Sharov V, White J, Li J, Liang W, Bhagabati N, et al. TM4: a free, open-source system for microarray data management and analysis. Biotechniques 2003;34:374–8.
[45] Flint HJ, Bayer EA, Rincon MT, Lamed R, White BA. Polysaccharide utilization by gut bacteria: potential for new insights from genomic analysis. Nat Rev Microbiol 2008;6:121–31.
[46] Tong M, Li X, Wegener Parfrey L, Roth B, Ippoliti A, Wei B, et al. A modular organization of the human intestinal mucosal microbiota and its association with inflammatory bowel disease. PLoS One 2013;8:e80702.
[47] Trompette A, Gollwitzer ES, Yadava K, Sichelstiel AK, Sprenger N, Ngom-Bru C, et al. Gut microbiota metabolism of dietary fiber influences allergic airway disease and hematopoiesis. Nat Med 2014;20:159–66.
[48] Segain JP, Raingeard de la Bletiere D, Bourreille A, Leray V, Gervois N, Rosales C, et al. Butyrate inhibits inflammatory responses through NFkappaB inhibition: implications for Crohn's disease. Gut 2000;47:397–403.
[49] den Besten G, van Eunen K, Groen AK, Venema K, Reijngoud DJ, Bakker BM. The role of short-chain fatty acids in the interplay between diet, gut microbiota, and host energy metabolism. J Lipid Res 2013;54:2325–40.

[50] Petersson J, Schreiber O, Hansson GC, Gendler SJ, Velcich A, Lundberg JO, et al. Importance and regulation of the colonic mucus barrier in a mouse model of colitis. Am J Physiol Gastrointest Liver Physiol 2011;300:G327–33.

[51] Moco S, Candela M, Chuang E, Draper C, Cominetti O, Montoliou I, et al. Perspectives for systems biology approaches for IBD personalized care: emphasis on gut microbial metabolic activities. Inflamm Bowel Dis 2014;20(11):2104–14. http://dx.doi.org/10.1097/MIB.0000000000000116.

[52] Candela M, Turroni S, Biagi E, Carbonero F, Rampelli S, Fiorentini C, et al. Inflammation and colorectal cancer, when microbiota–host mutualism breaks. World J Gastroenterol 2014;20:908–22.

[53] Furusawa Y, Obata Y, Fukuda S, Endo TA, Nakato G, Takahashi D, et al. Commensal microbe-derived butyrate induces the differentiation of colonic regulatory T cells. Nature 2013;504:446–50.

Variation at HLA-DRB1 is associated with resistance to enteric fever

Enteric fever affects more than 25 million people annually and results from systemic infection with Salmonella enterica serovar Typhi or Paratyphi pathovars A, B or C1. **Dunstan et al.** (Nature Genet 2014; doi:10/1038/ng.3143) conducted a genome-wide association study of 432 individuals with blood culture–confirmed enteric fever and 2,011 controls from Vietnam. We observed strong association at rs7765379 (odds ratio (OR) for the minor allele = 0.18, P = 4.5×10^{-10}), a marker mapping to the HLA class II region, in proximity to HLA-DQB1 and HLA-DRB1. The authors replicated this association in 595 enteric fever cases and 386 controls from Nepal and also in a second independent collection of 151 cases and 668 controls from Vietnam. Imputation-based fine-mapping across the extended MHC region showed that the classical HLADRB1*04:05 allele (OR = 0.14, P = 2.60×10^{-11}) could entirely explain the association at rs7765379, thus implicating HLADRB1 as a major contributor to resistance against enteric fever, presumably through antigen presentation